The Contrasting Oceanography of the Rhodes Gyre and the Central Black Sea

Alec F. GAINES, Graham M. COPELAND
Strathclyde University, Department of Civil Engineering,
Glasgow-SCOTLAND
a.f.gaines@strath.ac.uk
Yeşim ÇOBAN-YILDIZ
BOTAŞ International Limited, BTC Pipeline Operator, Haydar Aliyev Marine Terminal,
Adana-TURKEY
Emin ÖZSOY
Middle East Technical University, Institute of Marine Sciences,
İçel-TURKEY
Alexander M. DAVIE
Edinburgh University, Department of Mathematics and Statistics,
Edinburgh-SCOTLAND
Sergey K. KONOVALOV
Marine Hydrophysical Institute, NASU, Sevastopol, UKRAINE

Received 08.12.2004

Abstract

The Rhodes Gyre, a prominent feature of the oceanography of the eastern Mediterranean, is modelled as a vertical, continuous flow, cylindrical reactor illuminated during the day at its upper end. If the Gyre is supposed to be in a steady state whilst the concentrations, C, of a chemical are being measured, the nett rate of formation or consumption of the chemical is given by $-w\delta C/\delta z + u\delta C/\delta r$, where w is the upward velocity of the water in the vertical, z , direction and u is the velocity of the water in the radial, r, direction. The behaviour of w and u is analysed to show that the Gyre may be used as a field laboratory in which rates of chemical change may be derived from depth profiles together with values of the surface velocities of the Gyre waters.

In contrast, the central Black Sea is modelled as an ideal, strongly stratified sea in which the nett rates of formation or consumption of chemicals under steady state conditions are given by $D_\sigma d^2C/d\sigma^2$, where σ is the water density and D_σ is an eddy diffusion coefficient. Computations reveal that, given better knowledge of its eddy diffusion coefficients, the Black Sea can also be treated as a field laboratory where rates of reaction mediated by bacteria may be derived from depth profiles.

Key words: Rhodes Gyre, Black Sea, Modelling, Rates of reaction, Water density.

Introduction

Chemical oceanography strives to determine the reactions, and indeed their mechanisms, occurring at all locations and depths of the world ocean. Currently chemical oceanographers determine 'depth profiles', that is the concentrations of interacting chemicals and the population densities of phytoplankton as a function of depth at selected locations. The usefulness of the data is increased if the measurements are repeated at least seasonally for a number of years. This data-set is complemented by determinations of the physical oceanography at the

same depths and locations. Such measurements permit the formulation of hypotheses relating the concentrations of the different chemicals and the growth of phytoplankton. These hypotheses are usually non-quantitative, which makes it difficult to proceed further. Neither the rates of chemical reactions nor the rates of phytoplankton growth are commonly measured and straightforward interpretation of the depth-profiles is frequently inhibited by the advent of 'intermediate layers' of anomalous sea-water. Descriptions of the chemical and biochemical processes occurring in a sea would be much more complete were the 'water columns' to resemble chemical engineering reactors. Serendipitously, such a major simplification of physical oceanography occurs twice in the seas around Turkey. The 2 circumstances occur in dissimilar seas and involve contrasting chemical reactors. In the central Black Sea it has been found (Tuğrul et al., 1992) that, to a first approximation, chemical concentrations are functions solely of the water density, σ. In other words, concentrations of chemicals are constant in layers of equal density, isopycnals, right across the central basin though the isopycnals may be far from horizontal. In later sections we shall examine the mathematical consequences of this simplification.

Whereas the centre of the Black Sea is moderately fertile, in general, with one notable exception, the open sea in the eastern Mediterranean is a desert. The exception is an anticlockwise Gyre of water 10-50 km in radius somewhat south of Rhodes. The rotation of this column of water raises chemicals from the sea-bed towards the surface and, in so doing, encourages the growth of phytoplankton. The density, temperature and salinity of the water within the Gyre are essentially constant. In complete contrast to the central Black Sea most of the water column is well mixed. Indeed, the height of the Gyre being at least a kilometre, the swirling column of water forms a well stirred, vertical, continuous flow, biochemical reactor illuminated—during the day—at its upper end. We shall now show that the consequent mathematics appears interestingly simple.

The Rhodes Gyre

The Rhodes Gyre

The Rhodes Gyre, a distinct vertical cylinder of eastern Mediterranean water to the south of the island of Rhodes, rotates anticlockwise, the rotation presumably being a result of the wind driven basin circulation and the interaction of the Mid-Mediterranean Jet and the Asia Minor Current as they pass over the Rhodes Trench (Figure 1). The rotation causes water, comparatively rich in nutrients, to rise from the bottom of the sea to the surface and in consequence the Gyre is much more fertile than the rest of the eastern Mediterranean. The oceanography of the Gyre has been well studied (Özsoy et al., 1991, 1993; Theocharis et al., 1993; Yılmaz et al., 1994, 1999; Ediger et al., 1999; Napolitano et al., 2000). Our problem is to determine the rates of the chemical reactions that occur throughout the Gyre from the distribution of soluble chemicals and the vertical velocity of the sea-water. Figure 2 portrays typical depth profiles in the Gyre.

Napolitano et al. (2000) give references to previous explorations of the Gyre and describe how depth profiles may be simulated by the numerical integration of a sequence of coupled partial differential equations making use of the Princeton Ocean Model (Mellor, 1990). The model emphasises the importance of vertical eddy diffusion coefficients and the rates of change of all biological species are assumed to follow from Michaelis-Menten equations.

Figure 2 shows the water in the Rhodes Gyre to possess a rather uniform temperature, salinity and density. Unlike in previous computer simulations the Gyre will be regarded as a continuous flow reactor (Figure 3). It will be assumed that, the water in the Gyre being essentially homogeneous, the variation of its density, σ, with depth, z, can be neglected.

The Model

Given a system of cylindrical polar coordinates, z (measured vertically downwards; z is zero in the upper surface, the air-sea interface of the Gyre), r and ϕ. The corresponding velocities of the water in this system are w (vertically upwards), u (radial) and v (at right angles to u – rotation). Assume w, u and v to be independent of ϕ, that is, assume circular (axial) symmetry. Consider an elemental torus (annulus) (Figure 3):

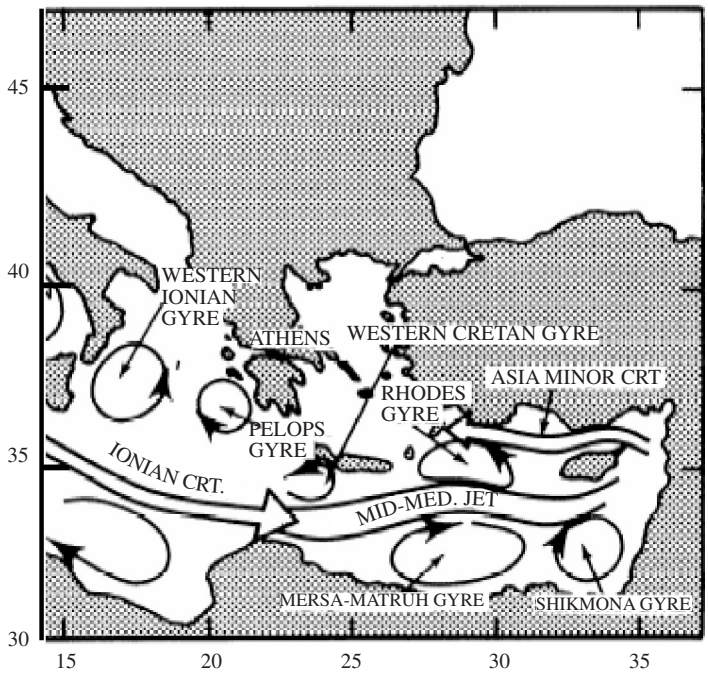

Figure 1. Schematic of surface circulation features in the Eastern Mediterranean Basin (from Roussenov et al., 1995).

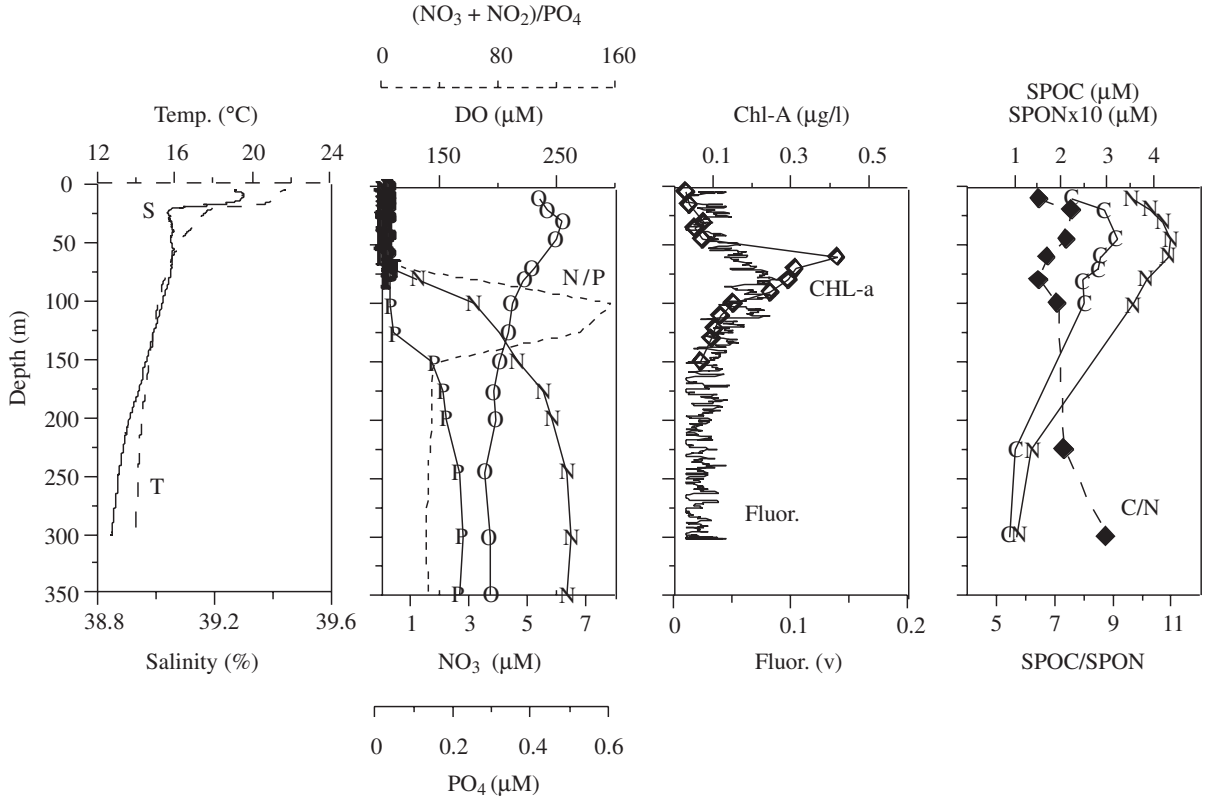

Figure 2. Depth profiles in the Rhodes Gyre (Autumn 1999) of Salinity (S) Temperature (T), Dissolved Oxygen (DO), NO_3 (N), PO_4 (P) and N/P ratio (N/P), Chlorophyll-a (CHL-a), Fluorescence (Fluor), suspended particulate organic carbon (C), nitrogen (N) and SPOC/SPON ratio (C/N).

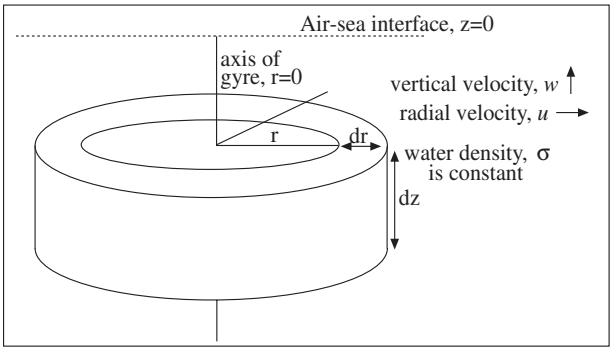

Figure 3. Elemental torus in the Rhodes Gyre assuming circular-axial symmetry.

Conservation of water mass (equation of continuity):

The flux of water mass in the upward direction is

$$-2\pi r(dr)\sigma w + 2\pi r(dr)\sigma(w + \delta w/\delta z(dz))$$

$$= 2\pi r\sigma\delta w/\delta z.dzdr$$

The radial flux of water mass perpendicular to the z axis is

$$2\pi r\sigma u(dz) - 2\pi(r + dr)\sigma(dz)(u + \delta u/\delta r(dr))$$

$$= -2\pi\sigma(r\delta u/\delta r + u)drdz$$

The total flux of water mass must be zero.

Therefore,

$$2\pi r\sigma\delta w/\delta z.dzdr = 2\pi\sigma(r\delta u/\delta r + u)drdz,$$

$$\delta w/\delta z = \delta u/\delta r + u/r$$

or

$$r\delta w/\delta z = \delta ru/\delta r \qquad (1)$$

Conservation of soluble chemicals:

One proceeds similarly to the conservation of water mass.

Let the concentration in the Gyre of a selected soluble chemical be $C(z, r)$.

Then the vertical flux of the selected soluble chemical is

$$-2\pi r(dr)Cw + 2\pi r(dr)(w + \delta w/\delta zdz)(C + \delta C/\delta zdz)$$

$$= 2\pi rdrdz(w\delta C/\delta z + C\delta w/\delta z)$$

The radial flux of the selected chemical perpendicular to the z axis is

$$2\pi urCdz - 2\pi(r + dr)(C + \delta C/\delta rdr)(u + \delta u/\delta rdr)dz$$

Therefore, if $R(C)$ is the rate of change (nett rate of formation or consumption per unit volume) of the selected chemical due to chemistry or biochemistry,

$$2\pi rdrdzdC/dt = R(C)2\pi rdrdz$$
$$+2\pi rdrdz(w\delta C/\delta z + C\delta w/\delta z)$$
$$-2\pi C(r\delta u/\delta r + u)drdz - 2\pi ru\delta C/\delta rdrdrdz$$

or

$$rdC/dt = rR(C)+r(w\delta C/\delta z+C\delta w/\delta z)-C(r\delta u/\delta r+u)$$
$$-u\delta C/\delta r$$

Whence, from (1)

$$dC/dt = R(C) + w\delta C/\delta z - u\delta C/\delta r \qquad (2)$$

and in a steady state

$$R(C) = -w\delta C/\delta z + u\delta C/\delta r \qquad (2a)$$

Equation (1) shows that along the axis, where r = 0, u must be zero (unless $\delta w/\delta z$ be infinite). Therefore along the axis Eqs. (2) and (2a) are particularly simple since the term $u\delta C/\delta r$ disappears.

Equation (1) is the standard equation of continuity of a fluid expressed in cylindrical polar coordinates with circular (axial) symmetry. It has been derived here from first principles so as to emphasise that Eqs. (2) and (2a) take radial (and rotational) flow into account even along the axis where the equations appear one dimensional.

It is Eq. (2a) that one wishes to use. If one assumes the Gyre to be in a steady state throughout the duration of measurements, then Eq. (2a) shows how R(C), and thus the chemical oceanography within the Gyre may be determined from the derivatives of C with respect to depth. Depth profiles of C are and have been measured routinely (Figure 2). It should be remarked here that whereas previous models of the Rhodes Gyre (e.g., Napolitano et al., 2000) have described depth profiles in terms of eddy diffusion coefficients, the derivation of Eqs. (1), (2) and (2a) has ignored eddy diffusion of C within the homogeneous water column and R(C) is given in terms of the velocities of the water, w and u. In fact the neglect of eddy diffusion is only apparent since the effects of turbulence are incorporated into R(C) itself. To illustrate, suppose R(C) to be the rate of interaction (reaction) of two species 1 and 2. Then R(C) may be expressed,

$$R(C) = P_1 P_2 C_1 C_2, \tag{3}$$

where P_1 is the probability of an entity (molecule) of species 1 colliding with an entity of species 2; P_2 is the probability of the 2 colliding entities interacting (reacting) and C_1 and C_2 are the concentrations of the 2 species. Depending on the nature of the interaction P_2 may depend on such parameters as temperature, light intensity and the energy of the collision. P_1, and the energy of the collision will depend on the nature and intensity of the turbulence.

Since w is positive, Eq. (2a) shows R(C) to be negative when C increases with depth down the axis of the Gyre. Thus nitrate concentrations increase with depth, with nitrate being consumed everywhere along the axis of the Gyre, particularly within the nitracline. This is rather obvious. Consideration of phytoplankton growth along the axis of the Gyre is more interesting.

The related depth profiles of phytoplankton, chlorophyll-a fluorescence and particulate organic carbon within the Gyre are all very similar in increasing with depth to a maximum towards the bottom of the euphotic zone and subsequently decreasing with further increase in depth (Figure 2). Thus, in the surface of the euphotic zone where δ C/δz is positive, phytoplankton populations increase with nitrate and phosphate concentrations at increasing depth along the axis of the Gyre whereas light intensity diminishes. It is tempting to suppose one is observing nutrient limited growth of phytoplankton. At the bottom of the euphotic zone, below the phytoplankton maximum, where $\delta C/\delta$z is negative, light intensity continues to diminish and phytoplankton populations decrease although nitrate and phosphate concentrations increase markedly. It appears that phytoplankton growth is light limited along this region of the axis.

If Eq. (2a) pertains to phytoplankton populations, the previous description of phytoplankton growth implies that in the surface waters of the Gyre phytoplankton cells are sedimenting—at least down the axis—but in the bottom of the euphotic zone the cells are being borne upward by the upwelling water of the Gyre. Clearly, further work is necessary to confirm this interpretation. The phenomena are subtler in that some species of phytoplankton can modify their density so as to approach the surface during hours of darkness and phytoplankton populations may vary diurnally in consequence.

To quantify R(C) one needs estimates of w and u. It appears impractical to determine w in the field. One therefore needs a method of calculating w from other observable parameters. If the water in the Gyre is assumed to be not only incompressible but also inviscid, calculation of w involves application of the Euler or Bernoulli equations to the flow in the Gyre. However, significant information can be obtained from Eq. (1).

Suppose one writes

$$w = w(z)w(r)$$

and

$$u = u(z)u(r).$$

Then, from Eq. (1),

$$w(r) = (Sr)^{-1} d\{ru(r)\}/dr, \tag{4}$$

where S is a separation constant.

Equation (1) shows u to be zero along the axis of the Gyre and one expects $u(r)$ to become zero when r is large. Thus, $u(r)$ passes through a maximum. Consequently Eq. (4) indicates $w(r)$ and hence w to change sign at the value of r at which $d\{ru(r)\}/dr$ is zero. At a sufficient distance from the centre of the Gyre there is no longer upwelling, and the water flows downwards to the bottom.

The simplest mathematics assumes the angular momentum to be confined to the axis of the Gyre and, accordingly, w and u to be derived from a 'potential' Φ such that

$$Del^2(\Phi) = 0$$

and

$$w = -\delta\Phi/\delta z \text{ and } u = \delta\Phi/\delta r$$

relationships that satisfy Eq. (1).

Under these circumstances one finds

$$w = Ak\{exp(kz) - exp(-kz)\}J_O(kr) \qquad (5a)$$

and

$$u = Ak\{exp(kz) + exp(-kz)\}J_1(kr), \qquad (5b)$$

where k is a separation constant and J_O and J_1 are zero and first order Bessel functions.

A is a constant given by the boundary conditions.

Note that when r is zero along the axis of the Gyre, the zero and first order Bessel functions are unity and zero, respectively.

When kz is small

$$w = 2Ak^2zJ_O(kr) \qquad (6a)$$

and

$$u = 2AkJ_1(kr) \qquad (6b)$$

and u does not vary with depth when kz is small.

Boundary conditions and characterisation of the model

At the surface the Bessel function J_1(kr), giving the radial velocity of the Gyre, is zero at the centre of the Gyre, increases to a maximum and decays again to zero as we have discussed following Eq. (4). Suppose future field experiments indeed show the radial velocities of the surface waters to fit a Bessel function J_1 (kr). The effective radius r_O of the Gyre may then be defined as the radius where u is zero. That is, where $kr_O = 3.835$, since $J_1(3.835) = 0$. Thus $k \sim 4/r_O = 2\text{-}4x10^{-4}$ m^{-1} if, as observation suggests, r_O is usually 1-20 km. kz is likely to be small and Eq. (6a) to be applicable down to depths of at least 750 m. Equation (6a) indicates w to become zero and change sign where kr is 2.405 (J_O (2.405) = 0). At this value of r upwelling ceases and this may be a more practical definition of the boundary of the Gyre. The absence of upwelling and the commencement of downwelling suggest the edge of the Gyre will be indicated as a region of great infertility but, since we have ignored eddy diffusion, the model cannot be expected to be accurate when w is near to zero.

It may, therefore, be more accurate to determine k from the distance from the central axis at which the radial velocity is a maximum. This maximum value of the radial velocity occurs when the Bessel function J_1 (kr) is a maximum, that is when kr = 1.845. Thus, measurement of the maximum value of u enables A to be determined from Eq. (6b). Equations (6) may now be used to compute w and u.

Rates of consumption of nitrate and phosphate

Equations (2a) and (6a) show the biochemical rates of change of nitrate and phosphate down the axis of the Gyre to a depth of 300m to be calculable from

$$R = -\text{constant } z\delta C/\delta z, \qquad (7)$$

the constant being determinable from measurements of radial velocities in the surface water. This is exciting chemical oceanography.

Table 1 shows the relative rates of consumption—in arbitrary units of nitrate and phosphate concentrations—down the axis of the Gyre during the autumn of 1999 calculated from Figure 2. Unfortunately, the corresponding population densities of phytoplankton were not measured but Table 1 includes relative rates of consumption per unit of Particulate Organic Carbon (POC). The Table suggests, perhaps surprisingly, that the phytoplankton cells consumed most actively at around 125-150 m depth.

The above analysis, including the calculation of Table 1, will remain valid in the top 300 m of the Gyre even if the assumptions underlying Eqs. (5) are incorrect—that is, should experiment show u not to be a first order Bessel function of r—providing the radial velocity of the Gyre, u, is independent of depth. Under these circumstances let

$$u = a_1r + a_2r^2 + a_3r^3 + \ldots, \qquad (8a)$$

whence, from Eq. (1),

$$w = 2a_1 + 3a_2r + 4a_3r^2 + \ldots. \qquad (8b)$$

The constants a_n can be determined experimentally from measurements of the radial velocities in

surface waters and thus w may be computed at known depths and used to calculate rates of change (Eq. (2a)).

The ability to derive rates of consumption from Eq. (2a) should enable future work to relate these quantities to the light intensities in the water column and the concentrations of nutrients. In other words, future work should derive quantitative expressions for the rates of consumption by phytoplankton cells inhabiting the Gyre.

The Black Sea

An ideal, strongly stratified sea

Quite generally the distribution of the concentration, C, of a soluble chemical or nutrient throughout a sea is described by the partial differential equation:

$$dC/dt = D_X \delta^2 C/\delta x^2 + D_Y \delta^2 C/\delta y^2 + \delta/\delta z(D_Z \delta C/\delta z) + u\delta C/\delta x + v\delta C/\delta y + w\delta C/\delta z + R(C). \quad (9)$$

Equation (9) is the law of conservation of mass for the chemical; the first 3 terms on the right-hand side express the diffusion of the chemical, the next 3 terms express its advection, whilst R(C), which may be a function of C, represents the nett rate of change of concentration due to all chemical, biochemical and geochemical reactions[1].

It is a major objective of chemical oceanography to determine R(C) from Eq. (9) by the utilisation of measured depth profiles. Usually it is very difficult to accomplish this objective.

Certain seas cease to be well stirred in the depth direction, z, and become stratified. That is, their temperature, water density, and chemical concentrations vary significantly with depth. Here we define an ideal, strongly stratified sea by the equation

$$C = C(\sigma). \quad (10)$$

That is, the concentration of any selected chemical in the sea can be expressed as a function of the water density, σ, only (Figure 4).

In such an ideal, strongly stratified sea Eq. (9) simplifies markedly and one finds quite rigorously (Appendix A)

$$D_\sigma d^2C/d\sigma^2 + R(C) = 0, \quad (11a)$$

where

$$D_\sigma = D_X(\delta\sigma/\delta x)^2 + D_Y(\delta\sigma/\delta y)^2 + D_Z(\delta\sigma/\delta z)^2. \quad (11b)$$

Table 1. Relative rates of consumption (arbitrary units), $z\delta C/\delta z$, in the Rhodes Gyre, Autumn, 1999.

Depth (m)	z $\delta NO_3/\delta z$	z $\delta NO_3/\delta z$ per unit of POC	z $\delta PO_4/\delta z$	z $\delta PO_4/\delta z$ per unit of POC
0	0	0	0	0
25	0.004	small	0.0025	small
50	0.575	small	0.0050	small
75	5.12	1.97	0.009	0.00335
100	7.08	4.16	0.0232	0.014
125	4.5	2.8	0.31875	0.20
150	3.0	2.0	0.4	0.27
175	2.22	1.64	0.175	0.13
200	1.96	1.63	0.13	0.11
225	1.845	1.68	0.10	0.092
250	1.475	1.38	0.075	0.07
275	1.24	1.20	0.063	0.061
300	1.11	1.11	0.060	0.06

[1]Note that, in starting from (9) we have ignored the interesting problem of the calculation of the eddy diffusion coefficients D_X, D_Y and D_Z and approximated (simplified) by supposing the currents u, v and w and the eddy diffusion coefficients D_X and D_Y to be constants. The eddy diffusion coefficient in the depth direction, D_Z, is a function of z.

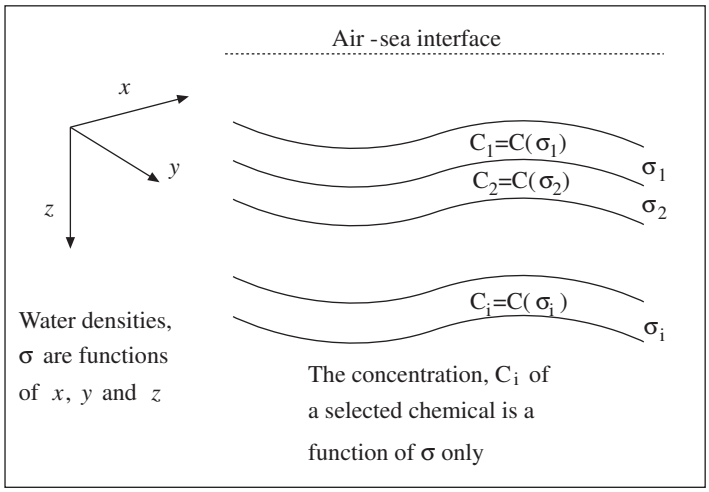

Figure 4. Model of a strongly stratified sea.

Notice that Eq. (9) and (11.2) are expressed in partial derivatives but Eq. (11.1) is an ordinary differential equation. One sees Eq. (10) to imply the concentration C(σ) to be in a steady state in terms of water density, its variation with σ being controlled by a straightforward diffusion equation.

Equation (11.1) appears to be novel; it shows that if, in an ideal, stratified sea one measures depth in terms of water density, the distribution of chemical concentrations follows a simple one dimensional diffusion equation in which (Appendix A) advection terms do not occur (though advection may appear indirectly by changing the water density in the x, y and z directions). Naturally, understanding of the distribution of water density within a strongly stratified sea still requires 3-dimensional modelling of the basin.

Equation (11.1) is important in that it shows that in any ideal, strongly stratified sea the nett rates of consumption or formation of chemicals or nutrients, R(C), may be obtained from numerical differentiation of the appropriate depth profile, a much simpler operation than manipulating Eq. (9). We give examples in the next section. The only physical parameter occurring in Eq. (11.1) is the eddy diffusion coefficient, D_σ, and Eq. (11.2) implies that complete understanding of this parameter will require 3-dimensional modelling of the basin. Diffusion coefficients in the x and y directions generally being much larger than those in the vertical, z direction (Kolmogorov 4/3 law), Eq. (11.2) shows these parameters to dominate D_σ (despite the fact that partial derivatives $\delta\sigma/\delta$x and $\delta\sigma/\delta$y are often smaller than $\delta\sigma/\delta$z), when the isopycnals slope. That is, if Eq. (9) were to be valid, vertical mixing would be greatest in those regions of the sea where such topography as sea mounts and shelf breaks cause the isopycnals to slope in the x or y directions.

In the middle of an ideal, strongly stratified sea where water density varies solely with depth, Eqs. (11.1) and (11.2) reveal R(C) to be a function of water density and zones in which R(C) represents a source or a sink are delineated by the isopycnals at which the second derivatives of concentration with respect to water density are zero.

The Black Sea

The previous section introduced a new equation, (11.1), that enables the nett rates of formation or consumption of chemicals in any strongly stratified sea to be determined from the second derivatives of their depth profiles provided depths are described in terms of water density. Table 2 uses observations of the Black Sea to illustrate the procedure, its limitations and the conclusions that can be drawn.

The Black Sea, being the world's largest anoxic basin, its chemical oceanology has received much study (Oğuz et al., 1996, 2000; Özsoy and Ünlüata, 1997). Earlier quantitative simulations of the depth profiles of chemicals in the Black Sea often assumed concentrations to be a function of depth, z, but not of x or y (e.g., Brewer and Murray, 1973; Oğuz et al., 1996). However, Tuğrul et al. (1992) demonstrated Eq. (10) to be valid to a first approximation throughout the central Black Sea and consequently it is Eq. (11.1) which should describe the depth profiles.

Equation 11.2 indicates vertical mixing to be

greatest where the shelf slopes at the boundaries of the basin, which is where, as intuition suggests, land-based inputs of nutrients mix vertically into the water-column. Subsequent mixing occurs 'horizontally' from the boundary to the centre of the basin along isopycnal surfaces. Detailed mixing processes are reviewed by Özsoy and Ünlüata (1997)—see their Figures 18 and 22 for examples. Here we apply Eq. (11.1) to the depth profiles of the silicate, ammonium and hydrogen sulphide concentrations observed in the centre of the basin by Russian oceanographers and collated by Brewer (1971). Unfortunately, more recent and probably more accurate observations do not extend to the bottom of the basin although one can discuss the recent nitrate profiles observed by R/V Knorr and R/V Bilim. While Eqs. (11) are inevitably an approximation to the behaviour of the central Black Sea, the simplicity of Eq. (11.1) implies that its numerical integration will be significantly more accurate than numerical manipulation of Eq. (9).

Table 2 presents depth profiles of the concentrations of silicate, ammonium and hydrogen sulphide deduced from observations (Brewer, 1971) from 5 stations above the abyssal plain of the central Black Sea. The Table considers depths in excess of a water density of 16.0 where Eq. (10) was seen to apply; the

Table 2. Variation of dissolved silicate, ammonium and hydrogen sulphide concentrations with water density. Calculated* from Brewer and Murray (1973).

σ	16.0	16.1	16.2	16.3	16.4	16.5	16.6	16.7	16.8	16.9	17.0	17.1
S	3.2	3.2	3.2	3.2	3.15	3.15	3.15	3.1	3.1	3.0	2.95	2.85
$(d\sigma/dz)^2$	150	110	86.5	64	46	30	18	10.6	5.1	2.2	0.6	0.25
SiO_4	50.2	53.2	57.5	63.2	69.1	75.3	82.5	91.3	101.3	112.6	126.2	141.3
$d^2SiO_4/d\sigma^2$	57.5	132	135	30	18	80	141	157	145	219	155	150
$F_{SiO4}+$	8.6	14.5	11.7	1.9	0.83	2.4	2.5	1.7	0.74	0.48	0.09	0.04
F_{SiO4}	3.0	5.8	7.0	1.5	0.83	2.9	3.3	2.3	1.0	0.65	0.11	0.03
NH_4	0.45	1.12	1.77	3.03	4.35	6.37	9.63	14.8	22.5	32.7	45.0	60.0
$d^2NH_4/d\sigma^2$	0.5	3.2	22	35	75	118	192	256	265	265	265	265
$F_{NH4}+$	0.08	0.35	1.9	2.2	3.45	3.5	3.45	2.7	1.4	0.58	0.16	0.07
F_{NH4}	0.03	0.14	1.1	1.8	3.5	4.2	4.5	3.8	1.9	0.79	0.18	0.06
H_2S	0.03	0.25	1.03	2.45	5.13	13.2	25.5	40.7	60.5	88.8	129	182.8
$dH_2S/d\sigma^2$	19.7	44.5	76	172	484	435	271	454	872	1141	1313	1600
$F_{H2S}+$	3.0	4.9	6.6	11.0	22.2	13.1	4.9	4.8	4.4	2.5	0.82	0.4
F_{H2S}	1.0	2.0	3.9	8.8	22.2	15.7	6.3	6.7	6.2	3.4	0.95	0.36

S = Surface area of isopycnal in 10^{11} m^2; $(d\sigma/dz)^2$ are in units of $(\sigma)^2 10^{-6} m^{-2}$.

SiO_4, NH_4 and H_2S denote the average concentrations* of nutrient sampled at the isopycnal in micromoles.

$F_X+$is the product $(d\sigma/dz)^2 d^2C/d\sigma^2$ in μmoles per m^2 x 10^{-3};

F_X are the respective rates of consumption at the isopycnal in μmol/s x 10^{-8} calculated from Eq. (11.1) using the eddy diffusion coefficients given by Samodurov and Ivanov (1998). The total rates of consumption over each isopycnal are obtained by multiplying F_X by S.

*Depth profiles are averages from 5 locations (Locations 1439, 1445, 1446, 1462 and 1466 (Brewer, 1971)) over the abyssal plain in the central Black Sea where concentrations appeared to satisfy Eq. (10). These averages were smoothed using a simple 3-point formula. Smoothed values are shown in Table 2. The second derivatives shown in the Table were computed from the smoothed values using standard formulae generated by fitting a polynomial to 5 equally spaced (σ = 0.05) points (Milne, 1949). Calculations of errors showed no improvement in accuracy to result from the use of either smaller intervals of σ or of more sophisticated formulae for smoothing or calculating second derivatives.

Table also shows the second derivatives of the concentrations with respect to water density. (Procedures for the necessary numerical computations are indicated in the legend.) Although the concentrations of silicate, ammonium and hydrogen sulphide all increase monotonically to reach their maximum values at the sea-bed, the 3 depth profiles are different as is obvious from the marked differences in their second derivatives with respect to water density (Table 2).

In the middle of the Black Sea, above the abyssal plain, water density varies very little in the horizontal x or y directions. In order to determine the eddy diffusion coefficient D_σ so as to calculate the nett rates of formation or consumption in Eq. (11.1) one needs to know only the square of the derivative of water density with respect to depth together with the eddy diffusion coefficient D_Z in the z direction. Table 2 shows the results of computations of the square of the derivative of water density with respect to depth. $\delta\sigma/\delta$z increases from the surface to a maximum in the pycnocline and then diminishes. As the water density increases from 16.0 to 17.1 values of $(\delta\sigma/\delta\ z)^2$ decrease over 100-fold, becoming zero at the sea-bed. Accordingly D_σ and therefore R(C) (Eq. (11.1)) also become zero at the sea-bed, and the high concentrations of dissolved silicate, ammonium and hydrogen sulphide observed at the base of the water column are due, not to a constant rate of production, R(C), but to equilibrium of the chemicals at the sea-bed in the bottom convection layer (Özsoy and Ünlüata, 1997) with those in the surface sediment. The depth profiles of the rates of production, R(C), given by the products of the second derivatives with $(\delta\sigma/\delta z)^2$ and D_Z are also shown in Table 2. The greatest uncertainty in these values arises from the uncertainty in our knowledge of the magnitudes of the eddy diffusion coefficients D_Z, which vary markedly with depth. As yet we have no straightforward experimental routine for determining D_Z and we have used the values computed by Samodurov and Ivanov (1998) in obtaining Table 2. Multiplication of the values of R by the areas of each isopycnal gives the depth profiles of the total rates of production.

Dissolved silicate in the central Black Sea

From Table 2 one may conclude that in the surface, at water densities of less than 14.5, $d^2SiO_4/d\sigma^2$ is negative and dissolved silicate is consumed, presumably by dinoflagellates and diatoms (Grill, 1970; Brewer, 1971). At these depths $\delta\sigma/\delta$z and D_Z are both of the order of 10^{-4} m^2/s (Brewer and Murray, 1973) and the rates of consumption may be relatively large. It is difficult, however, to determine $d^2SiO_4/d\sigma^2$ accurately and the stratified sea model may not apply to surface waters. When the water density lies between 14.6 and 15.2 $d^2SiO_4/d\sigma^2$ is essentially zero and there is no nett rate of dissolution or consumption of silicate in this part of the water column. When water densities exceed 16.0 $d^2SiO_4/d\sigma^2$ is positive and there is continual dissolution of particulate silicate, maximum rates of dissolution occurring at water densities of about 16.2 and 16.6 (Table 2).

At larger water densities the rates of dissolution decrease to zero at the sea-bed. As with ammonium and hydrogen sulphide the total rate of dissolution throughout the Black Sea may readily be calculated by integrating the dissolution at each isopycnal over depth but this is hardly worth doing until one can be certain of the estimates of the eddy diffusion coefficients.

Ammonium in the central Black Sea

Above the pycnocline it is difficult to compute $d^2NH_4/d\sigma^2$ accurately. Below the pycnocline until the water density reaches about 16.0 $d^2NH_4/d\sigma^2$ is zero and there is no nett consumption or formation of ammonium. When water densities exceed 16.0, $d^2NH_4/d\sigma^2$ increases. The corresponding rate of formation of ammonium increased to a maximum value at a water density of about 16.6 (Table 2) and subsequently decreased to zero at the sea-bed.

Hydrogen sulphide in the central Black Sea

The second derivative with respect to water density of the concentration of hydrogen sulphide is zero when the water density is less than about 15.9. The depth profiles show no evidence of either formation or consumption of hydrogen sulphide at such water densities. When the water density exceeds 15.95 the second derivative is positive and nett hydrogen sulphide is formed, presumably due to the bacterial reduction of sulphate. The rate of formation reaches a maximum at a water density of about 16.4 (Table 2). At larger water densities the rate decreases to a plateau at water densities of 16.6-16.8 and then declines to zero at the sea-bed.

Nitrate in the central Black Sea

Figure 5 recapitulates the depth profiles of nitrate concentrations in the Black Sea during cruises by R/Vs Knorr and Bilim together with rough computations of the second derivatives of nitrate concentrations with respect to water density. Nitrate concentrations are very low in the surface waters of the central Black Sea, increase to a maximum value in the pycnocline at water densities of around 15.4 and then decline, becoming zero at water densities between 16.0 and 16.5 so that it is not necessary to consider concentrations in the deep anoxic waters. Eddy diffusion coefficients are not known accurately at these depths but the second derivatives of the concentrations with respect to water density provide significant information. Clearly, in the region of the maximum nitrate concentration $d^2NO_3/d\sigma^2$ is negative and, in fact Figure 5 shows this second derivative to be negative throughout the depths in which nitrate concentrations are measurable. The obvious interpretation is that nitrate concentrations carried into the Black Sea by the rivers are mixed rapidly along isopycnal surfaces and throughout the 'nitrate region' the ion is consumed (Eq. (11.1)). To determine the rates of consumption and subsequently clarify the processes involved one needs values of D_Z. Such values are difficult to obtain accurately in the pycnocline where D_Z changes rapidly. The second derivative of the nitrate concentrations with respect to water density changes sign and becomes positive only in the tails of the nitrate distribution and only in these limited regions is there nett production of nitrate. The rate of production will be greater in the tail toward the surface since this is where the eddy diffusion will be greater.

Distribution of bacteria

This analysis has shown that in the 1970s rates of dissolution of silicate and of the formation of ammonium and hydrogen sulphide had maximum values at water densities between 16.2 and 16.6. At the bottom of the water column where the concentrations of these chemicals were largest, the nett rates of dissolution and formation were zero. Clearly, the rates of the dissolution and formation reactions had no simple relationship to the concentrations of the relevant chemicals. The formation of hydrogen sulphide and ammonium being mediated by bacteria (Price, 1976; Jorgensen et al., 1991), one surmises that the rates of formation in the water column will be proportional to the population densities of the relevant bacteria and accordingly these population densities had their maxima at water densities of about 16.4 (hydrogen sulphide) and 16.6 (ammonium). This suggests a direction for future research. If the source of the silica which is dissolving is biogenic, that is, if the silica is derived from the cell walls of dinoflagellates and diatoms, one may again suppose the rate of this remineralisation to depend on a population of bacteria. However, the silica may dissolve subsequent to its formation from clay minerals (Price, 1976). The large populations of bacteria adsorbed on the seabed, much larger than the populations in the water column (Price, 1976), presumably suffice for the reactions of dissolution and formation to be sufficiently fast as to generate equilibria at the interface between the sediment and the water.

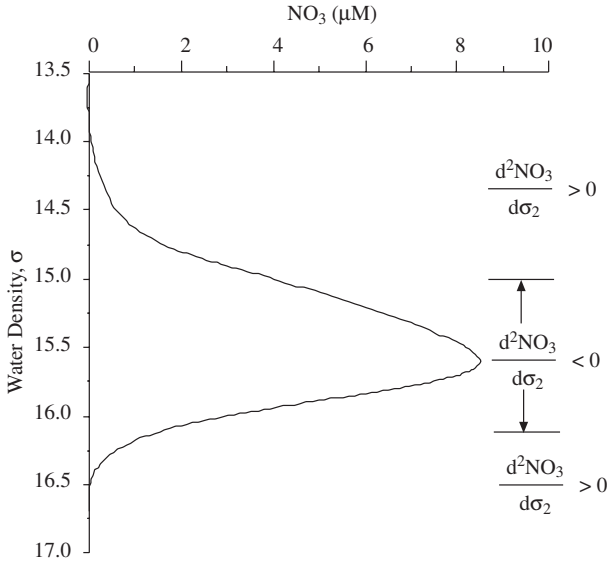

Figure 5. Nitrate (NO_3) profile in the central Black Sea based on Tuğrul et al. (1992).

Acknowledgements

This work formed a small part of NATO's Science for Stability Programme in the Black Sea.

References

Brewer, P., "Hydrographic and Chemical Data from the Black Sea". Unpublished manuscript, Woods Hole Oceanographic Institution, Technical Report No. 71-65, Mass. USA. 1971.

Brewer, P. and Murray, J.W., "Carbon, Nitrogen and Phosphorus in the Black Sea", Deep-Sea Research, 20, 803-818, 1973.

Ediger, D., Tuğrul, S., Polat, C.S., Yılmaz, A. and Salihoğlu, I., "Abundance and Elemental Composition of Particulate Matter in the Upper Layer of the North Eastern Mediterranean", In: The eastern Mediterranean as a laboratory basin for the assessment of contrasting ecosystems (P. Malonotte-Rizzoli and V.N.Eremeev, Eds.), Kluwer Acad. Publs. 241-266, 1999.

Grill, EV, "A Mathematical Model for the Marine Dissolved Silicate Cycle", Deep-Sea Research, 17, 245-266, 1970.

Jorgensen, B.B., Fossing, H., Wirsen, C.O. and Jannasch, H.W., "Sulfide Oxidation in the Anoxic Black Sea Chemocline", Deep-Sea Research, 38, S1083-S1103, 1991.

Mellor, G.L., "User's Guide for a Three Dimensional, Primitive Equation Numerical Ocean Model", Progress in Atmospheric and Ocean Science, Princeton University Press, Princeton, New Jersey, 1990.

Milne, W.E., "Numerical Calculus", Princeton University Press and Oxford University Press, 1949.

Napolitano, E., Oğuz, T., Malanotte-Rizzoli, P., Yılmaz, A. and Sansone, E., "Simulations of Biological Production in the Rhodes and Ionian Basins of the Eastern Mediterranean", Journal of Marine Systems, 24, 277-298, 2000.

Oğuz, T., Ducklow, H., Malanotte-Rizzoli, P., Tuğrul, S., Nezlin, N. and Ünlüata, U., Simulations of annual plankton productivity cycle in the Black Sea by a one-dimensional physical-biological model. Journal of Geophysical Research, 101, 16585-16599, 1996.

Oğuz, T., Ducklow, H.W. and Malanotte-Rizzoli, P., "Modelling Distinct Vertical Biogeochemical Structure of the Black Sea". Dynamical Coupling of the Oxic, Suboxic and Anoxic Layers, Global Biogeochem Cycles, 14, 1331-1352, 2000.

Özsoy, E., Hecht, A., Ünlüata, U., Brenner, S., Oğuz, T., Bishop, J., Latif, M.A. and Rosentraub, Z., "A Review of the Levantine Basin Circulation and Its Variability During 1985-1988", Dyn. Atmos. Oceans. 15, 421-456, 1991.

Özsoy, E., Hecht, A., Ünlüata, U., Brenner, S., Sur, H.İ., Bishop, J., Oğuz, T., Rosentraub, Z. and Latif, M.A., "A Synthesis of the Levantine Basin Circulation and Hydrography", Deep-Sea Research, 40, 1075-1119, 1993.

Özsoy, E. and Ünlüata, U., "Oceanography of the Black Sea: A Review of Some Recent Results", Earth Science Reviews, 42, 231-272, 1997.

Price, N.B., "Chemical Diagenesis in Sediments", Chapter 30 in Volume 6 of Chemical Oceanography (J.P. Riley and R. Chester, Eds), Acad. Press, 1976.

Roussenov, V., Stanev, E., Artale, V. and Pinardi, N., "A Seasonal Model of the Mediterranean Sea General Circulation", Journal of Geophysical Research, 100, C7, 13515-13538, 1995.

Samodurov, A.S. and Ivanov, L.I., "Process of Ventilation of the Black Sea Related to Water Exchange Through the Bosphorus, in Ecosystem Modelling as a Management Tool for the Black Sea" (L.I. Ivanov and T. Oğuz, Eds.) Kluwer Acad. Publ. Volume 2, 221-235, 1998.

Theocharis, A., Georgopoulos, D., Lascaratos, A. and Nittis, K., "Water Masses and Circulation in the Central Region of the Eastern Mediterranean, Eastern Ionian, South Aegean and Northwestern Levantine", 1986-1987, Deep-Sea Research II, 40, 1121-1142, 1993.

Tuğrul, S., Başẗurk, Ö., Saydam, C. and Yılmaz, A., "Changes in the Hydrochemistry of the Black Sea Inferred from Water Density Profiles", Nature, 359, 237-239, 1992.

Yılmaz, A., Ediger, D., Başẗurk, Ö. and Tuğrul, S., "Phytoplankton Fluorescence and Deep Chlorophyll Maxima in the North Eastern Mediterranean", Oceanol. Acta, 17, 69-77, 1994.

Yılmaz, A. and Tuğrul, S., "The Effect of Cold and Warm Core Eddies on the Distribution and Stoichiometry of Dissolved Nutrients in the North Eastern Mediterranean", J. Marine Systems, 16, 253-268, 1999.

Appendix A.

If $C = C(\sigma)$ *(10) and Figure 4.*

Then $\delta C/\delta x = dC/d\sigma\delta\sigma/\delta x,$, $\delta C/\delta y = dC/d\sigma\delta\sigma/\delta y$ *and* $dC/\delta z = dC/d\sigma\delta\sigma/\delta z$.

So that $\delta^2 C/\delta x^2 = \delta\ /\delta x\ \{dC/d\sigma\delta\sigma/\delta x\} = d^2 C/d\sigma^2\ (\delta\sigma/\delta x)^2 + dC/d\sigma\delta^2\sigma/\delta x^2$

With similar expressions for $\delta^2 C/\delta y^2$ *and* $\delta^2 C/\delta z^2$.

Substituting these expressions into Eq. (9) one obtains

$dC/dt = [\{D_X(\delta\sigma/\delta x)^2 + D_Y(\delta\sigma/\delta y\ )^2 + D_Z(\delta\sigma/\delta z)^2\}d^2 C/d\sigma^2 + \{D_X\delta^2\sigma/\delta x^2 + D_Y\delta^2\sigma/\delta y^2 +$

$\delta\ /\delta z(D_Z\ \delta\sigma/\delta z) - u\delta\sigma/\delta x - v\delta\sigma/\delta y - w\delta\sigma/\delta z\}dC/d\sigma + R(C)$ *(12).*

The expression in curly brackets multiplying $dC/d\sigma$ *on the right hand side of Eq. (12) is seen to be* $d\sigma/dt$ *(*$C = \sigma$ *in Eq. (9)). Thus, the expression yields* $d\sigma/dt\ dC/d\sigma$, *which is* dC/dt *and cancels with the left-hand side of Eq. (12). Hence in the steady state implied by Eq. (10), the velocities u,v and w disappear and Eq. (12) simplifies to Eqs. (11.1) and (11.2).*